

Materials Science inc. Nanomaterials & Polymers

Supramolecular Structure of Temperature-Dependent Polymeric Hydrogels Modulated by Drug Incorporation

Margareth K. K. D. Franco,^[a] Anderson F. Sepulveda,^[b, c] Aryane A. Vigato,^[b, c] Alisson Oshiro,^[b] Ian Pompermayer Machado,^[d] Ben Kent,^[e, f] Daniel Clemens,^[e] Fabiano Yokaichiya^{+, * [e]} and Daniele Ribeiro de Araujo^{+* [b, c]}

Ploxamers or Pluronic[®] (PL) have been described as promising pharmaceutical and cosmetics matrices. Herein, we have explored the structural organization of hydrogel formulations composed of PL F-127 and PL L-81, considering their different hydrophilic-lipophilic balances and interactions with an anti-migraine drug, sumatriptan succinate (SMT). Hydrogels phase organizations were investigated by X-ray diffraction (XRD) and Small Angle Neutron Scattering (SANS) to establish the relationship between structural features and drug release modulation. XRD analysis revealed very low intensity peaks for hydrogels containing SMT due to the presence of small amounts of SMT as crystalline form, which is an evidence of drug incorporation into hydrogels. At physiological temperature, a structural transition from lamellar to hexagonal was observed after SMT incorporation. In addition, SANS patterns displayed a distorted hexagonal structure, (calculated $q_2 >$ experimental q_2), indicat-

ing the presence of a comprised structure compared to a perfect hexagonal assembly. This structural shift however have no influence on the drug release mechanism, allowing the SMT molecules to access the micellar and intermicellar hydrophilic spaces, with release mechanism dependent on the drug diffusion ($R^2 = 0.998 \geq 0.986$) from the hydrogel to the medium and release constant (K_{rel}) values from 9.8 to 14.7%.h⁻¹; 31.5 to 39.1%.h^{-1/2}; 0.84 to 1.2%.h⁻ⁿ for Zero-order, Higuchi and Korsmeyer-Peppas models, respectively. Using SMT as a drug model, it could be concluded that the drug access to the micellar/intermicellar hydrophilic spaces can be modulated by interplaying the polarity of binary PL-based hydrogels. Therefore, drug release constants and mechanisms will be then dependent on the hydrogels physico-chemical and structural properties, which determine the drug diffusion from the hydrogel to the release medium.

1. Introduction

Stimuli responsive polymeric materials are able to change their structural organization upon some environmental settings (temperature, light, pH etc), forming systems with wide applicability in Biological, Materials and Environmental fields.

Also called as smart polymers, they have been extensively reported in the literature due to their self-assembly capability in aqueous medium, leading to distinct phase-behaviors in response to environmental conditions.^[1–5] In general, pH-sensitive systems have been frequently studied, specially chitosan-based systems (vinyltrimethoxy silane cross-linked chitosan/polyvinylpyrrolidone; 2-aminobenzamide cross-linked chitosan; carboxymethyl chitosan-polyoxometalate) for drug-delivery and tissue regeneration purposes.^[6–11]

Regarding to thermosensitive systems, one of the main classes of stimuli-responsive copolymers are poloxamers or Pluronic[®] (PL), smart materials highly responsive to temperature. Pluronic[®] (PL) are copolymers composed of polyethylene oxide (PEO) and polypropylene oxide (PPO) blocks linked as an A–B–A type structure. Due to their amphiphilic properties, PEO and PPO monomers self-assemble in aqueous medium above the critical micellar concentration (CMC), forming micelles with a hydrophobic core (PPO units) and a hydrophilic corona (PEO units), which allow the incorporation of both hydrophobic and hydrophilic compounds, as well as the differential interaction with other surfactants that induce changes on PL transition properties according to their distribution into micelles microenvironment.^[12] In addition, PL display thermoreversible properties, attributed to the dehydration of PPO core units while the hydrophilic PEO corona remains hydrated, which promotes micellae self-assembly into different

[a] Dr. M. K. K. D. Franco

Energy and Nuclear Research Institute, São Paulo, SP, Brazil

[b] A. F. Sepulveda, A. A. Vigato, Dr. A. Oshiro, Prof. D. R. de Araujo⁺

Human and Natural Sciences Center, Federal University of ABC, Santo André, SP, Brazil

E-mail: daniele.araujo@ufabc.edu.br
draraujo2008@gmail.com

[c] A. F. Sepulveda, A. A. Vigato, Prof. D. R. de Araujo⁺

Drugs and Bioactives Delivery Systems Research Group – SISLIBIO, Federal University of ABC. Av. dos Estados, 5001. Bl. A, T3, Lab. 503-3. Bangú. Santo André-SP, Brazil

[d] I. P. Machado

Department of Fundamental Chemistry, Institute of Chemistry, University of São Paulo, São Paulo, SP, Brazil

[e] Prof. B. Kent, Dr. D. Clemens, Prof. Fabiano Yokaichiya⁺


Institute for Soft Matter and Functional Materials, Helmholtz-Zentrum Berlin für Materialien, Berlin, Germany

E-mail: fabiano.yokaichiya@helmholtz-berlin.de

[f] Prof. B. Kent

School of Chemistry, University of New South Wales. Kensington, Australia.

[⁺] Both authors contributed equally to this original research.

 Supporting information for this article is available on the WWW under <https://doi.org/10.1002/slct.202001116>

phase structures (e.g. cubic, hexagonal, lamellar) at a sol-gel transition temperature ($T_{\text{sol-gel}}$). Therefore, micellae self-assembly forms gel materials, characterized by a partially rigid structure with high viscosity.^[13,14]

PL-based hydrogels are promising pharmaceutical and cosmetic matrices due to their low toxicity, low cost, and high malleability. Binary combinations of different types of PL highlight many possibilities regarding its supramolecular structure, increasing the potential for further biopharmaceutical applications. In fact, the use of smart polymeric materials with accurate physico-chemical characterization is essential for the design of new pharmaceutical formulations during the early stages of the development, since it is possible to establish a relationship between the supramolecular structure responsible for the best performance as drug-delivery system and the main factors involved in this process (temperature and pH-induced drug release, additives like other polymers and drugs).^[6-8,10-11]

However, literature studies on these polymeric systems lack on structural characterization, particularly regarding scattering techniques, which could provide important information on the structural phase organization, essential to improve physico-chemical stability and thus enhance therapeutic efficacy.^[15-17] In this context, Small Angle Neutron Scattering (SANS) is a powerful technique to understand the structural arrangements in the gels after incorporation of drugs with different physicochemical features.^[18-20] Combining the data provided by SANS and drug release analyses, it is possible to determine the gels' supramolecular structure under real conditions, e.g. physiological temperature and the dissolution medium used for pharmaceutical preparations, allowing to understand how the formation of different supramolecular structures can modulate their performance as drug-delivery systems.^[21]

In addition to the problem of the lack of structural characterization, it is worth noting that several studies discuss the chemical interactions between PL-based hydrogels structure and different drugs. A common result is that drug-polymer interactions induce changes on polymer self-assembly mechanisms.^[22] However, emphasis was given to biopharmaceutical features instead of the physical-chemical and structural characterization of the formulations. It is worth noting that detailed knowledge on the supramolecular structure of self-assembled PL-based systems is essential to understand how additives (e.g. other polymers and drugs) can modulate the phase organization and, consequently, the drug-delivery performance.^[15,16]

For example, SAXS patterns showed that PL-based hydrogels phase organizations were influenced by PL-L81, a hydrophobic PL (Hydrophilic Lipophilic Balance -HLB- value of 2), incorporation into PLF-127 (HLB=22) hydrogels, forming a binary system with transitions from lamellar (PLF-127) to hexagonal phase (PLF-127/PLL-81), from 25 to 37 °C and considering two final copolymers concentrations (18 to 20%). Also, systems containing PLL-81 showed lower drug release constant values. In this previous work, drug incorporation was also associated with hexagonal phase organization, but structural arrangements were similar to those observed in absence of drug.^[15] Similar results were also observed for the system

PLF-127/PLF-68, which transitions from lamellar to hexagonal were also observed.^[16]

In a recent study, it was reported different behaviors resulting from hyaluronic acid (HA) incorporation into the systems composed of PLF-108 (HLB=29), more hydrophilic compared to PLF-127, showing transitions type from Body Centered Cubic (BCC) to gyroid and/or from BCC to lamellar, as observed for the binary hydrogels (HA-PLF-127-PLF-108). However, those phase transitions were not associated to lower release constants, showing that the hexagonal phase organization seems to be essential for a sustained drug release performance.^[17]

In general, the hexagonal phase organization can facilitate the drug incorporation into the intermicellar spaces, possibly being the preferential structure for evoking low drug release constant values. On the other hand, the specific drug effects on hydrogel's supramolecular structure and its consequences on release mechanisms were not studied. Therefore, an investigation on the influence of drugs and other PL on hydrogel matrix supramolecular organization is essential to understand the drug release mechanisms and thus open new pathways for nanomedicines development.

The description of sumatriptan (SMT), used as drug model in this study, as an effective and well tolerated antimigraine drug was an important milestone for the therapy of migraine episodes, since SMT is precursor of triptan drugs. Several delivery systems have been proposed for SMT, e.g. micro-needles and patches.^[23-25] In addition, few studies were devoted to the development of gel-based formulations as hydrogels.^[15,26-27]

In this work, we explored structural organization of hydrogels composed of binary PL F-127 and PL L-81 formulations by Small Angle Neutron Scattering (SANS). In order to investigate the structural alterations after drug incorporation, SMT succinate, an effective and well-tolerated antimigraine drug, was chosen as a drug model. The SANS technique is able to access lower q range at different temperatures, which is essential to understand the local-scale drug effects on PL-based drug-delivery systems and their relationships with drug release mechanisms. By combining SANS data and *in vitro* release results, it is possible to state that the addition of SMT allowed the formation of a less distorted hexagonal structure at physiological temperature, which reduced the drug release constant values without changing the release mechanisms.

2. Results and Discussion

2.1. XRD profiles for PL-based formulations

The X-Ray Diffraction patterns were registered to initially characterize the influence of SMT in the crystal structure of 20% PL F-127 formulations (Figure 1). The XRD pattern for SMT succinate reveals a crystalline structure with several sharp diffraction peaks in the 7–40° range, which the high intensity ones are localized at around 16 and 21°. When analyzing the XRD patterns for PL formulations, one can observe the two characteristic diffraction peaks for the PL polymers at 19 and

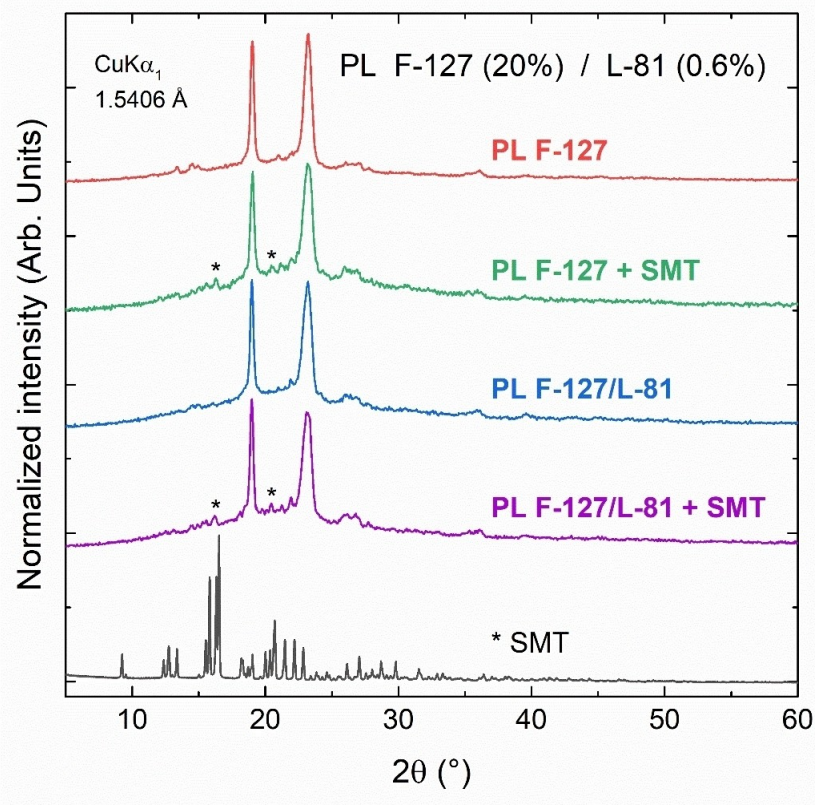


Figure 1. X-ray diffraction patterns for the sumatriptan succinate (SMT) and the formulations PL F-127 20 % and PL F-127/PL L-81 20/0.6%, without and with SMT.

23° and small intensity peaks at 16 and 21° just for SMT containing formulations, which are assigned to the SMT succinate. The low intensity of these peaks confirms that just a small amount of SMT is still on its crystalline form, meaning an efficient incorporation of the drug in the PL hydrogels.^[28–30]

2.2. SANS analysis: SMT incorporation evokes a distortion of the hydrogels hexagonal structure

Figure 2 shows the SANS patterns for the systems composed of PL F-127 and PL F-127/L-81, with and without the SMT, at different temperatures: 25 °C (storage temperature), 37 °C (physiological temperature) and 40 °C. For 18% PL F-127 systems in the presence of PL L-81, a lamellar phase organization structure was observed at 25 °C, before and after SMT incorporation (Figure 2, c–f). This lamellar structure remains stable up to 37 °C, but only for SMT-free hydrogels. After the drug incorporation, a structural transition from lamellar to hexagonal was observed at all measured temperatures (Figure 2 – b, d, f).

Considering that SMT presents low partition coefficient ($\log P=1.2$) and it is commercially available as succinate salt, the most probable mechanism for the SMT incorporation is that SMT interacts with the internal hydrogel structure, expelling water molecules from corona and/or intermicellar spaces

(implying a salting-out effect like),^[31] consequently changing the structure from lamellar to hexagonal. This agrees with previously reported SAXS results for the same hydrogel systems containing SMT succinate and the for PL F-127/F-68 formulations containing other salt-form drugs, e.g. ropivacaine hydrochloride,^[15–16] sodium naproxen, and sodium salicylate.^[19] In addition, former SANS studies highlighted the enhancement of the inter-micellar interactions according to the increase on temperature and salt concentration (especially sodium halides).^[32] In a similar manner, the effects of different flurbiprofen concentrations evoked changes on SANS patterns due to micelles attractive interactions and/or changes in the micellar structure.^[33]

Regarding to PL concentration effects, for 20% PL F-127 systems, hexagonal structure was found for all formulations at all temperatures, in the presence or absence of SMT (Figure 2B, a–f). It is worth noting that, considering the peak positions related to the hexagonal reflections (1,0), (1,1) and (2,0), the first (q_1 [1, 0]) and second (q_2 [1, 1]) peaks of an ideal hexagonal structure should follow the relation $q_2 = \sqrt{3}q_1$. Nevertheless, due to distortions of the hexagonal structure, as displayed in the SANS patterns (Figure 3), q_1 and q_2 position values deviate this relation, specially at 37 °C (Table 1). More precisely, calculated q_2 values are higher than the experimental q_2 for all samples, indicating that the PL formulations have a comprised

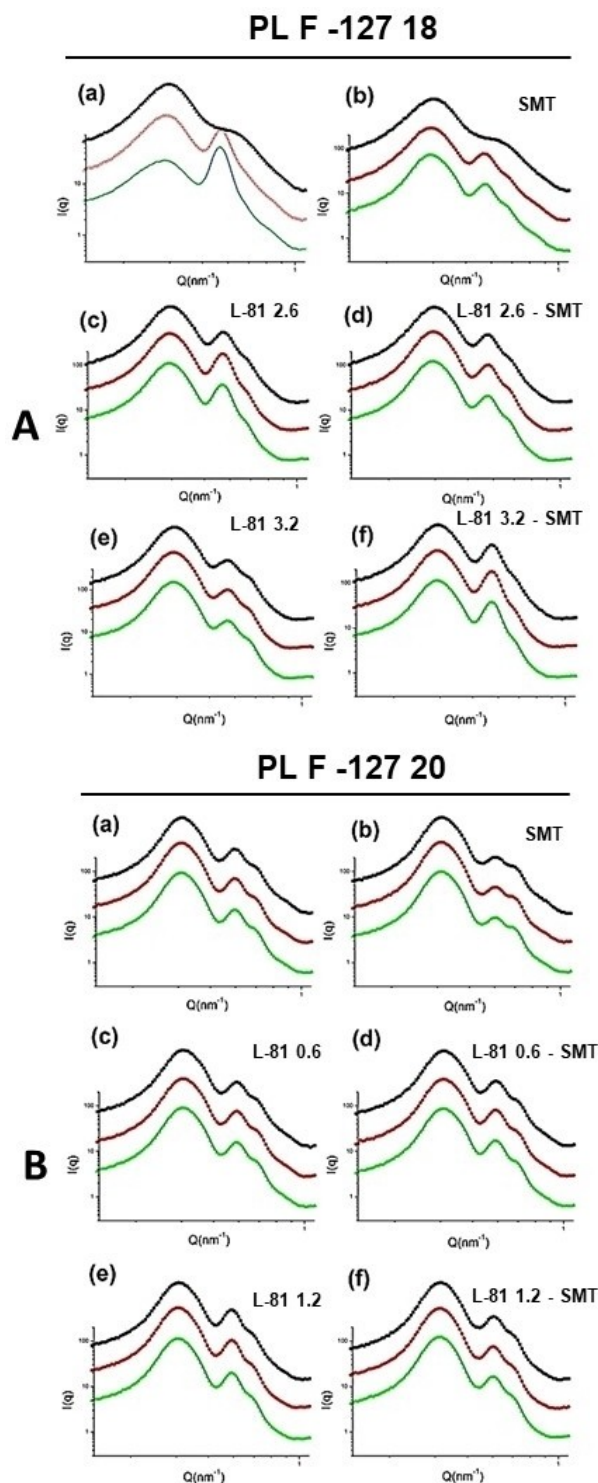


Figure 2. SANS scans obtained for PL F-127 18% (A) and 20% (B) systems for three temperatures (25 °C, 37 °C and 40 °C represented by black, red and green lines, respectively) at different L-81 concentrations, before and after SMT incorporation. Observe that for the unique PL F-127 18%, the system remains lamellar for all temperatures. Table 1 shows the measured q values under identified peaks.

structure in the d_{11} axis compared to a perfect hexagonal assembly (Figure 3). Then, at physiological temperature, the

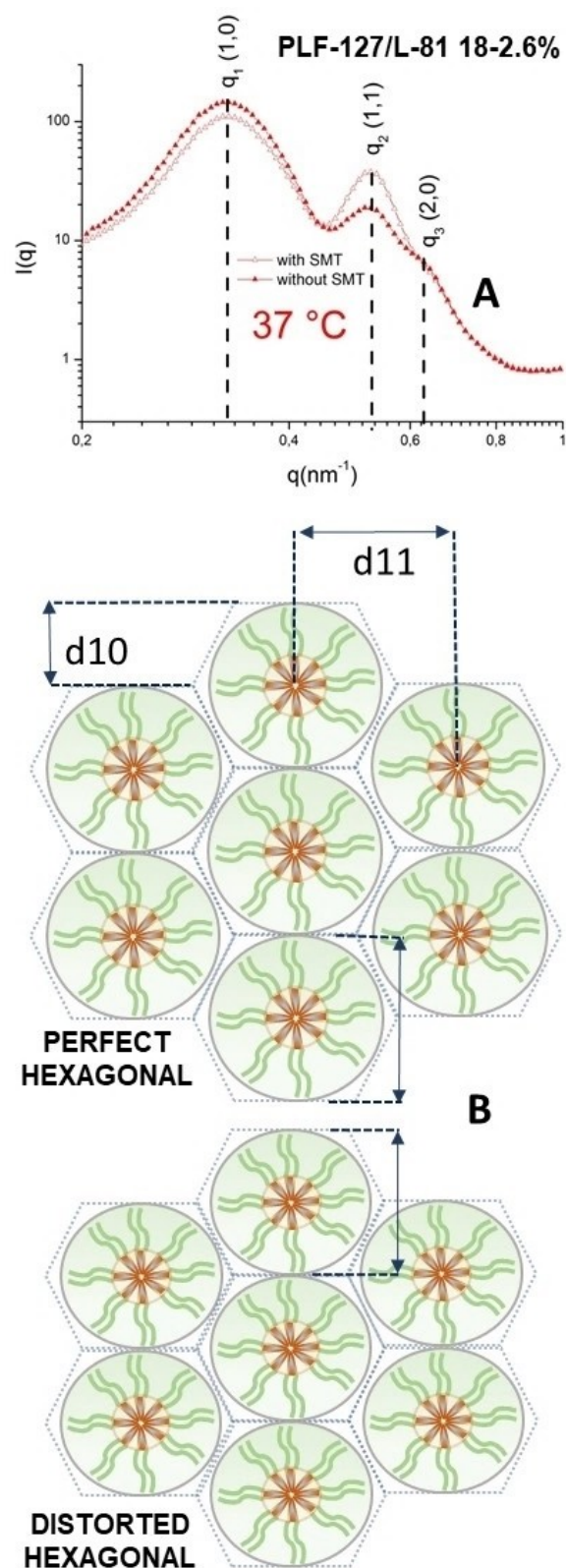


Figure 3. SANS patterns for PL F-127 18% + L-81 2.6% with and without SMT, showing a hexagonal structure at 37 °C (A) and schematic representation of a hexagonal structure for the binary system PL F-127/L81 + SMT: perfect (A) and distorted hexagonal structures (B). Measured q values are presented in Table 1.

Components PL F-127 (%)	PL L-81 (%)	SMT absence			SMT presence		
		q_1	q_2 theoretical	q_2 measured	q_1	q_2 calculated	q_2 measured
18	–	–	–	–	0,3293(4)	0.5703	0.518(3)
	2.6	0.3298(4)	0.5713	0.519(2)	0.3312(4)	0.5736	0.518(4)
	3.2	0.3272(3)	0.5667	0.506(4)	0.3283(4)	0.5686	0.522(3)
20	–	0.3459(4)	0.5992	0.541(4)	0.3491(4)	0.6047	0.534(5)
	0.6	0.3424(4)	0.5930	0.536(4)	0.3467(4)	0.6005	0.532(3)
	1.2	0.3429(4)	0.5940	0.539(4)	0.3502(3)	0.6066	0.544(3)

drug-delivery system available for *in vivo* effect displays a distorted supramolecular structure when compared to SMT-free hydrogels, an important feature to modulate the SMT succinate release rate.

For better understanding of the behavior of PL + SMT hexagonal distorted systems, the (q_2 measured)/(q_2 calculated) ratio was plotted as a function of PL L-81 concentration for the formulations containing 18 and 20% of PL F-127 (Figures 4A and 4B, respectively). For PL F-127 18% systems, the incorporation of L-81 leads to a higher distortion of the hexagonal structure (open circles), possibly due to differences on HLB between both polymers and changes on system hydration/dehydration process. However, when SMT is added to those formulations (filled circles), an opposite behavior is observed, *i.e.* the (q_2 measured)/(q_2 calculated) ratio increases, representing a less distorted hexagonal assembly. On the other hand, SMT addition increases the hexagonal distortion in the PL F-127 20% formulation structures at all temperatures while an increase of PL L-81 concentration reduces the hexagonal distortion, as a tendency of a more organized system formation. Those observations highlight the differential effects of the drug insertion into hydrogels, modulating the supramolecular structure distortion according to the PL matrix concentration. As reported by a recent study, the non-equilibrium effects are essential for designing the hydrogels biopharmaceutical properties (such as syringeability/injectability) and to predict the drug deposition into the crystalline PL matrices. Also, by investigating a range of PLF-127 (from 15 to 30%) the authors reported a coexistence of hexagonal and cubic structures into the same matrix. However, the effects of drugs incorporation were not studied.^[21]

In addition to previous results, SANS patterns were also obtained at very low q , as observed on Figure 5. For 18% PL F-127 samples a structure packing tendency is observed when

increasing the PL L-81 concentration on the formulations, specially at 37 °C (Figure 5). The packing of the hydrogel crystalline matrix was also enhanced after SMT succinate incorporation. For the 20% PL F-127 formulations, however, this behavior was not observed, *i.e.* the addition of PL L-81 and SMT had no significant effect on the density of hydrogels. Then, the drug insertion increased the driving forces for the PL F-127/L-81 binary system aggregation at low PL concentrations, in agreement of other results previously described for micellar systems composed of hydrophilic and hydrophobic polymers PL F-127, PL P84 and PL F108.^[34]

2.3. In vitro release studies and mechanisms

In vitro release profiles for SMT from PL F-127 isolated or associated to PL L-81 were obtained for all hydrogels. In general, SMT release percentages against time were modulated by PL F-127 and PL L-81 concentrations, being observed regular and gradual drug release profiles from hydrogels systems. Results are presented on Figure 6 and Table 2.

For hydrogels containing 18% PL F-127, the incorporation of L-81 reduced the drug released percentage from 90.2 ± 1.8 to 59.0 ± 4.2 % for PL F-127 and PL F-127/L-81, respectively, at 6 h ($p < 0.001$). Similar results were also observed for 20% PL F-127 systems, since lower drug released amounts were obtained after L-81 incorporation. The release profiles were then evaluated using mathematical models (Zero order, Higuchi, Hixson-Crowel and Korsmeyer-Peppas). Results from fittings showed higher release constant (K_{rel}) values for SMT from 18% PL F-127 hydrogels, compared to 20%. Additionally, the incorporation of L-81 reduced the K_{rel} , presenting more pronounced effects for the system PL F-127/L-81 (18/3.2) when compared to PL F-127/L-81 (20/1.2), as a result of the L-81

Formulations	Zero Order		Higuchi		Korsmeyer-Peppas		n
	K_0 (% \cdot h $^{-1}$)	R^2	K_H (% \cdot h $^{-1/2}$)	R^2	K_{kp} (% \cdot h $^{-n}$)	R^2	
PL F-127 (18)	14.7 ± 1.9	0.949	39.1 ± 3.2	0.989	0.88 ± 0.08	0.975	1.33
PLF-127/L-81 (18–2.6)	10.4 ± 1.1	0.970	32.8 ± 1.9	0.986	0.89 ± 0.03	0.985	1.09
PLF-127/L-81 (18–3.2)	9.8 ± 1.0	0.995	31.1 ± 2.5	0.998	0.98 ± 0.01	0.999	1.00
PL F-127 (20)	11.5 ± 1.4	0.954	37.6 ± 1.8	0.993	0.84 ± 0.06	0.982	1.19
PLF-127/L-81 (20–0.6)	8.7 ± 0.4	0.973	28.7 ± 0.4	0.989	1.23 ± 0.08	0.986	0.81
PLF-127/L-81 (20–1.2)	9.8 ± 0.5	0.971	31.5 ± 2.2	0.995	0.98 ± 0.05	0.994	1.01

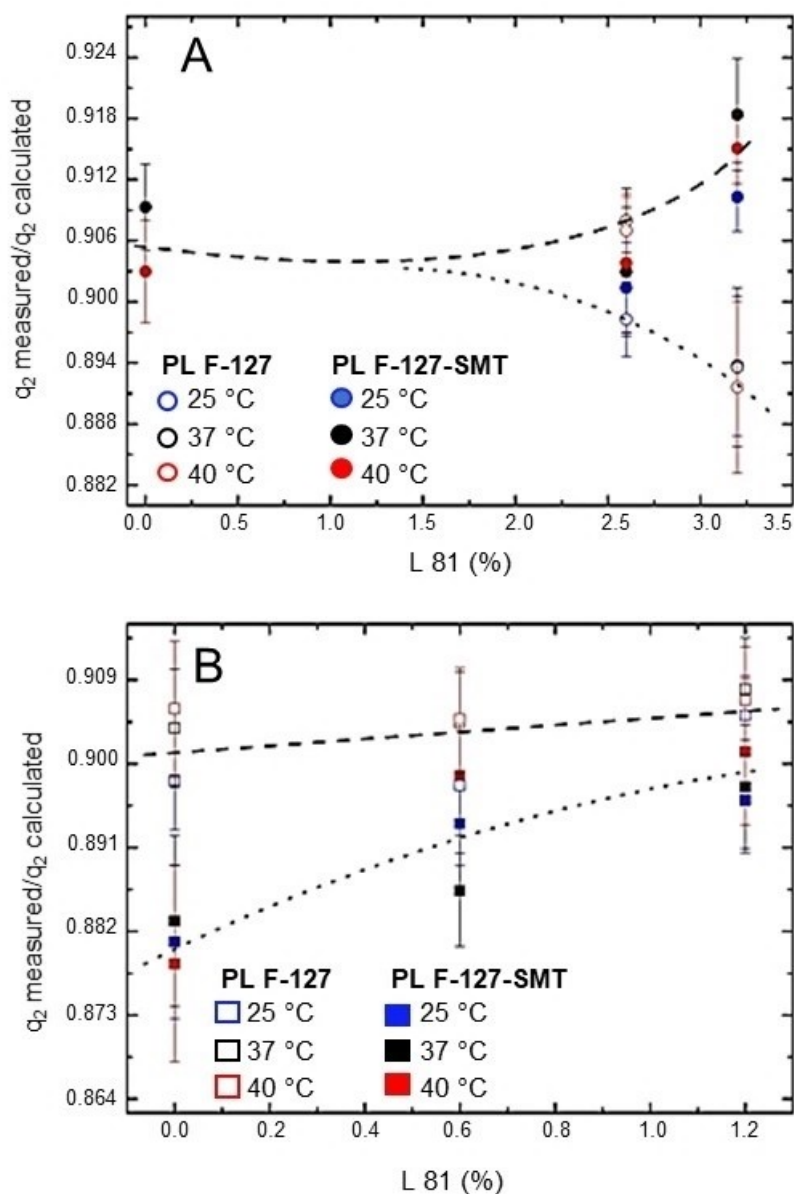


Figure 4. $(q_2 \text{ measured})/(q_2 \text{ calculated})$ ratio for PL F-127 18% (A) and 20% (B) systems before and after SMT incorporation, at three different temperatures.

presence, since both systems had the same PL final concentration (21.2%).

In general, the Krel values for hydrogel formulations were similar and followed the Higuchi model, where the best correlation coefficients intervals were obtained ($R^2 = 0.998 \geq 0.986$), as shown on Table 2. In this sense, it is possible to postulate that the release process is modulated by SMT diffusion, governed by Fick's law, from the hydrogel's matrices to the release medium. In fact, Fick's model reports that there is a drug concentration gradient directing the transference from the matrix to the external fluid. In the case of a subcutaneous injection, for example, the drug molecules diffuse from the hydrogels internal phase to the interface with the surrounding interstitial liquid.

In fact, gradual reduction on Krel values is observed in response to changes on final PL concentration (from 18 to 20.6%). However, at highest PL concentration (21.2%) the system tends to achieve a saturation, since no differences were observed on Krel.

Although the transition from a perfect to a distorted hexagonal phase organization, evoked by SMT by SANS analysis, this structural shift was not able to change the drug release mechanism. Therefore, at physiological temperature and in contact with biological fluids after injection, the PL-based hydrogels surface is rapidly dissolved and drug molecules can be possibly replaced by others located into the hydrogel's internal medium until the complete drug diffusion.^[35]

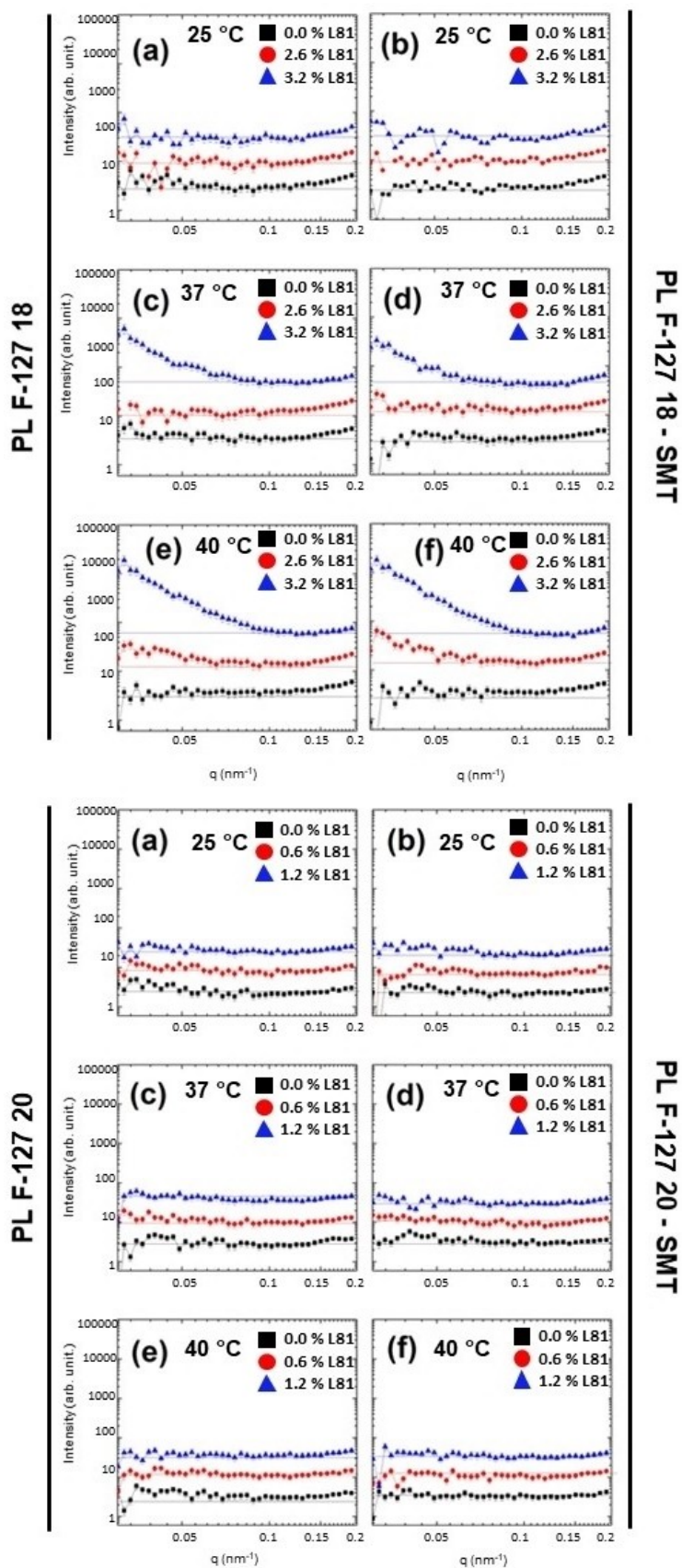


Figure 5. SANS scans for the systems composed of PL F-127 (a,c,e) and PL F-127-SMT (b,d,f) at different L81 concentrations and temperatures (25, 37 and 40 °C).

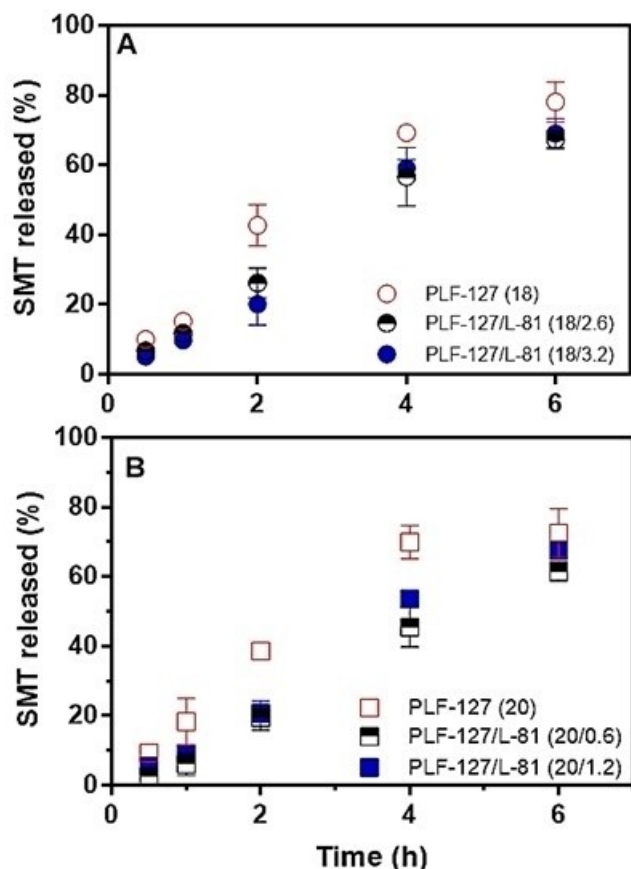


Figure 6. SMT *in vitro* release profiles from PL F-127 at 18% (A) and 20% (B) at different L81 concentrations ($n = 3/\text{formulation}$).

3. Conclusions

In this study, Small Angle Neutron Scattering (SANS) was employed to investigate the supramolecular structure of binary hydrogels systems, composed by two poloxamers (PL) with different polarities, PL F-127 and PL L-81. In general, the hydrogel formulations self-assemble into a hexagonal structure, exhibiting a distortion in the d_{11} axis compared to a perfect hexagonal assembly depending on the PL L-81 concentration. By combining SANS data and *in vitro* release results, we postulate that the addition of sumatriptan succinate (SMT) allowed a distorted hexagonal structure formation at physiological temperature, reducing the release constant values, without changing the release mechanisms. Moreover, at very low q range, no distorted agglomeration evoked by SMT incorporation was observed. In this context, it is necessary to highlight that this structural transformation is governed by not only temperature or PL concentration, but it is also dependent in the PL-type and its polarity.

In general, the hexagonal phase organization can facilitate the drug incorporation into the intermicellar spaces, being the preferential structure for evoking low drug release constant values. Herein, SANS analysis revealed that SMT incorporation evoked a distortion of the hydrogels hexagonal structure due to the promotion of micelle-micelle interactions. Then, at

physiological temperature and in the presence of drug, the delivery system available for possible *in vivo* effect displays a distorted supramolecular structure when compared to drug-free hydrogels, an important feature to predict the biopharmaceutical properties. By interplaying the polarity of binary PL-based hydrogels, SMT access to the micellar and intermicellar hydrophilic spaces can be modulated, and thus SMT release mechanism will be then dependent on the drug diffusion from the hydrogel to the release medium.

Supporting Information Summary

In this section are provided detailed information about hydrogels preparation, a description of physicochemical characterization and *in vitro* release assays for all formulations.

Acknowledgments

This research was supported by Coordenação de Aperfeiçoamento de Pessoal de Nível Superior (CAPES, Finance Code 001 and CAPES-PRINT - 88887.368001/2019-00), Conselho Nacional de Desenvolvimento Científico e Tecnológico (CNPq 309207/2016-9, 402838/2016-5, 307718/2019-0) and Fundação de Amparo à Pesquisa do Estado de São Paulo (FAPESP 2019/14773-8). The authors are also grateful to Prof. Hermi Felinto de Brito (Institute of Chemistry, University of São Paulo) and Maria Claudia França da Cunha Felinto (Nuclear and Energy Research Institute, São Paulo, SP, Brazil) for X-ray diffraction facilities.

Conflict of Interest

The authors declare no conflict of interest.

Keywords: Nanostructures · block copolymers · colloids · hydrogels · micelles

- [1] M. Angelinia, M. Bertoldo, B. Ruzicka, *Colloids Surf. A* **2017**, *532*, 389–396.
- [2] G. Le Fer, C. Le Coeura, J.–M. Guigner, C. Amiela, G. Voleta, *Polymer* **2019**, *171*, 149–160.
- [3] Y. J. Kim, Y. T. Matsunaga, *J. Mater. Chem. B* **2017**, *5*, 4307–4321.
- [4] A. Bordat, T. Boissenot, J. Nicolas, N. Tsapis, *Adv. Drug Delivery Rev.* **2019**, *138*, 167–192.
- [5] T. Shu, L. Hu, Q. Shen, L. Jiang, Q. Zhang, M. J. Serpe, *J. Mater. Chem. B* **2020**, *32*, 1–20.
- [6] N. Gull, M. Shahzad, K. Mqsood, K. Muhammad, T. Zahid, S. Butt, Z. Saba, S. Khalid, A. Islam, I. Sajid, R. Rafi, U. Khan, M. W. King, *Polym. Adv. Technol.* **2020**, *30*, 2414–2424.
- [7] N. Gull, S. M. Khan, M. T. Z. Butt, S. Khalid, M. Shafiq, A. Islam, S. Asim, S. Hafeeza, R. U. Khana, *RSC Adv.* **2019**, *9*, 31078–31091.
- [8] N. Gull, S. M. Khan, O. M. Butt, A. Islam, A. Shah, S. Jabeen, S. U. Khan, A. Khan, R. U. Khan, M. T. Z. Butt, *Int. J. Biol. Macromol.* **2020**, *162*, 175–187.
- [9] A. R. Karimi, G. Nikraves, F. Bayat, A. Khodadadi, M. Tarighatjoo, *ChemistrySelect* **2019**, *4*, 11378–11384.
- [10] Azizullah, A. Haider, U. Kortz, S. A. Joshi, J. Iqbal, *ChemistrySelect* **2017**, *2*, 5905–5912.
- [11] Azizullah, M. Al-Rashida, A. Haider, U. Kortz, S. A. Joshi, J. Iqbal, *ChemistrySelect* **2018**, *3*, 1472–1479.
- [12] J. Mishra, A. K. Mishra, *ChemistrySelect* **2019**, *4*, 4074–4082.
- [13] A. M. Bodratti, P. Alexandridis, *Expert Opin. Drug Delivery* **2018**, *15*, 1085–1104.

- [14] N. U. Khaliq, D. Y. Park, B. M. Yun, D. H. Yang, Y. W. Jung, J. H. Seo, C. S. Hwang, S. H. Yuk, *Int. J. Pharm.* **2019**, *556*, 30–44.
- [15] Oshiro, D. C. da Silva, J. C. de Mello, V. W. de Moraes, L. P. Cavalcanti, M. K. K. D. Franco, M. I. Alkschbirs, L. F. Fraceto, F. Yokaichiya, T. Rodrigues, D. R. de Araujo, *Langmuir*. **2014**, *30*, 13689–13698.
- [16] A. C. S. Akkari, J. Z. B. Papini, G. K. Garcia, M. K. K. D. Franco, L. P. Cavalcanti, A. Gasperini, M. I. Alkschbirs, F. Yokaichiya, E. de Paula, G. R. Tófoli, D. R. de Araujo, *Mater. Sci. Eng. C* **2016**, *68*, 299–307.
- [17] M. H. M. Nascimento, M. K. K. D. Franco, F. Yokaichiya, E. de Paula, C. B. Lombello, D. R. de Araujo, *Int. J. Biol. Macromol.* **2018**, *111*, 1245–1254.
- [18] M. Valero, C. A. Dreiss, *Langmuir*. **2010**, *26*, 10561–10571.
- [19] M. Valero, F. Castiglione, A. Mele, M. A. da Silva, I. Grillo, G. González-Gaitano, C. A. Dreiss, *Langmuir*. **2016**, *32*, 13174–13186.
- [20] V. Nguyen-Kim, S. Prévost, K. Seidel, W. Maier, A. K. Marguerre, G. Oetter, T. Tadros, M. Gradzielski, *J. Coll. Interface Sci.* **2017**, *477*, 94–102.
- [21] B. Shriky, A. Kelly, M. Isreb, M. Babenko, N. Mahmoudi, S. Rogers, O. Shebanova, T. Snow, T. Gough, *J. Coll. Interface Sci.* **2020**, *565*, 119–130.
- [22] Y. C. Chen, C. Y. Su, H. J. Jhan, H. O. Ho, M. T. Sheu, *Int. J. Nanomed.* **2015**, *10*, 7265–7274.
- [23] P. Ronnander, L. Simon, H. Spilgies, A. Koch, S. Scherr, *Eur. J. Pharm. Sci.* **2018**, *114*, 84–92.
- [24] Femenía-Font, C. Padula, F. Marra, C. Balaguer-Fernández, V. Merino, A. López-Castellano, S. Nicoli, P. Santi, *J. Pharm. Sci.* **2006**, *95*, 1561–1569.
- [25] Balaguer-Fernández, A. Femenía-Font, S. Del Rio-Sancho, V. Merino, A. López-Castellano, *J. Pharm. Sci.* **2008**, *97*, 2102–2109.
- [26] R. J. Majithiya, P. K. Ghosh, M. L. Umrethia, R. S. Murthy, *AAPS PharmSci-Tech* **2006**, *7*, 80–86.
- [27] U. C. Galgatte, A. B. Kumbhar, P. D. Chaudhari, *Drug Delivery* **2014**, *21*, 62–73.
- [28] V. Vyas, P. Sancheti, P. Karekar, M. Shah, Y. Pore, *Acta Pharm.* **2009**, *59*, 453–461.
- [29] V. Saxena, M. D. Hussain, *Int. J. Nanomed.* **2012**, *7*, 713–721.
- [30] W. Ali, A. C. Williams, C. F. Rawlinson, *Int. J. Pharm.* **2010**, *391*, 162–168.
- [31] L. Li, L. Hoon, L. Qiqiang, W. San, P. Jiang, *Polymer*. **2008**, *49*, 1952–1960.
- [32] J. P. Mata, P. R. Majhi, C. Guo, H. Z. Liu, P. Bahadur, *J. Colloid Interface Sci.* **2005**, *292*, 548–556.
- [33] S. Alexander, T. Cosgrove, T. C. Castle, I. Grillo, S. W. Prescott, *J. Phys. Chem. B*. **2012**, *116*, 11545–11551.
- [34] P. Singla, O. Singh, S. Chabba, V. K. Aswal, R. K. Mahajan, *Spectrochim. Acta A Mol. Biomol. Spectrosc.* **2018**, *191*, 143–154.
- [35] J. Siepmann, N. A. Peppas, *Int. J. Pharm.* **2011**, *418*, 6–12.

Submitted: March 19, 2020

Accepted: October 22, 2020